Journal of Japan Association for Earthquake Engineering, Vol. 24, No. 7, 2024

# PROBABILISTIC SEISMIC HAZARD ANALYSIS OF RESPONSE SPECTRA: TOWARD ADVANCED NATIONAL SEISMIC HAZARD MAPS FOR JAPAN

Yuji DOHI[1], Nobuyuki SHIGENO[2], Nobuyuki MORIKAWA[3], Hiroyuki FUJIWARA[4], Nobuoto NOJIMA[5] and Tomotaka IWATA[6]

[1] Member, Dr. Eng., Science and Technology Administrative Researcher, Ministry of Education, Culture, Sports, Science and Technology, Tokyo, Japan, dohi@bosai.go.jp
[2] Director for Earthquake Investigation, Ministry of Education, Culture, Sports, Science and Technology, Tokyo, Japan, nshigeno@mext.go.jp
[3] Member, Dr. Sc., Chief Researcher, National Research Institute for Earth Science and Disaster Resilience, Ibaraki, Japan, morikawa@bosai.go.jp
[4] Member, Dr. Sc., Manager, National Research Institute for Earth Science and Disaster Resilience, Ibaraki, Japan, fujiwara@bosai.go.jp
[5] Member, Dr. Eng., Professor, Department of Civil Engineering, Gifu University, Gifu, Japan, nojima.nobuoto.p6@f.gifu-u.ac.jp
[6] Dr. Sc., Professor, Disaster Prevention Research Institute, Kyoto University, Kyoto, Japan, iwata@egmdpri01.dpri.kyoto-u.ac.jp

**ABSTRACT**: The Earthquake Research Committee (ERC) of the Headquarters for Earthquake Research Promotion creates and updates national seismic hazard maps for Japan to help develop effective measures against earthquake hazards. The maps published by the ERC are based on seismic intensity; however, seismic hazard maps based on earthquake response spectra have become widespread in other countries and are used for engineering purposes, such as seismic design. In light of this, the Subcommittee for Evaluation of Strong Ground Motion under the ERC published a provisional probabilistic seismic hazard analysis (PSHA) of response spectra to contribute to discussions on the utilization of the PSHA for various needs, including engineering purposes. This paper discusses the provisional PSHA of response spectra, selection of ground motion prediction equations, evaluation conditions, evaluation results, utilization, and its future prospects. The development of the PSHA of response spectra is expected to continue, contributing to seismic design and serving as a basic resource for disaster prevention planning according to probability levels. The results of the provisional PSHA are anticipated to be discussed with various stakeholders, including those involved in disaster prevention, research, and the construction industry, to help develop the PSHA of response spectra.

**Keywords**: *Response spectra, Uniform hazard spectra, Ground motion prediction equation, Probabilistic seismic hazard analysis, Seismic hazard map*

## 1. INTRODUCTION

The Earthquake Research Committee (ERC) of the Headquarters for Earthquake Research Promotion (HERP) in Japan published the “National Seismic Hazard Maps for Japan (2005)” in March 2005[1)] to provide useful information for effective countermeasures against earthquake hazards for national and local public authorities and promote public awareness of disaster prevention and earthquake mitigation. The ERC continues to update the strong ground motion prediction method and subsurface structure models used in national seismic hazard maps, with the latest version being the “National Seismic Hazard Maps for Japan (2020)[2)]”. These maps, which are evaluated in terms of seismic intensity on the Japan Meteorological Agency scale, serve as valuable tools for disaster prevention planning, earthquake insurance premium rate determination, and other related endeavors[2)].

In other countries, seismic hazard maps based on earthquake response spectra have become widespread and are used for engineering purposes, such as seismic design. One example is the National Seismic Hazard Mapping Project of the U.S. Geological Survey, which began in the 1990s. Through this project, seismic hazard maps created based on a probabilistic approach were published for the U.S. Mainland in 1996, and subsequent maps for various U.S. regions have since been updated. In terms of the 2%, 5%, and 10% probability of exceedance in 50 years (PE50), 18 periods from 0.01 to 10.0 s focusing on 5% damped acceleration response spectra (pseudo-acceleration response spectra), peak ground acceleration, and peak ground velocity are available[3), 4)]. These seismic hazard maps were incorporated into the American Society of Civil Engineers 7 standard, Minimum Design Loads, and Associated Criteria for Buildings and Other Structures as the Maximum Considered Earthquake Ground Motion Map used for seismic design. Furthermore, these maps are used in the International Building Code, a common building code in the U.S. Other seismic hazard maps of response spectra based on probabilistic approaches have been published in Europe[5)], New Zealand[6)], and other countries.

In response to this, the HERP stated that “Although it has been pointed out that various data and analysis methods generated in the process of conducting long-term evaluations have potential to be used for a seismic design, it cannot be said they have not been sufficiently used,” and suggested a policy for developing seismic hazard maps based on response spectra for engineering purposes[7)]. Under this policy, the Subcommittee for Evaluation of Strong Ground Motion of the ERC and its Working Group on Advanced Seismic Hazard Maps developed the probabilistic seismic hazard analysis (PSHA) of response spectra and published its provisional edition (hereinafter referred to as the provisional PSHA) in November 2022[8)]. To contribute to the utilization of the PSHA for various needs and the accuracy improvement of the ground motion prediction equation (GMPE) and PSHA, the provisional PSHA mainly focuses on evaluation conditions and results. Focusing on the 5% damped acceleration response spectra (hereafter referred to as acceleration spectra) of the engineering bedrock of Tokyo, Nagoya, and Osaka, the hazard curves, uniform hazard spectra (UHS), and degree of influence (contribution factor) of earthquakes were computed.

In the following sections, we report the position of the provisional PSHA (Section 2), selection of the GMPEs (Section 3), evaluation conditions (Section 4), results (Section 5), discussions (Section 6), and conclusions (Section 7).

## 2. POSITION OF THE PSHA OF RESPONSE SPECTRA

This section outlines the seismic hazard maps published by the ERC and the position of the PSHA of response spectra.

The ERC publishes national seismic hazard maps and long-period ground motion hazard maps[9)–11)]. National seismic hazard maps consist of probabilistic and seismic hazard maps of specific seismic source faults. Probabilistic seismic hazard maps are generated by combining evaluations of long-term probabilistic earthquake occurrence with that of strong motions predicted at the time of earthquake occurrence. Based on the locations, magnitudes, and occurrence probabilities of all earthquakes that can be considered at present, the probability of the intensity of ground motions occurring within the target period exceeding a certain value by at least one degree at each site can be evaluated. Probabilistic seismic hazard maps show the distribution of the values obtained from the evaluation. Specifically, the peak velocity on the engineering bedrock is derived based on an attenuation relation using the shortest distance from the target site to the fault plane, then multiplying the derived value by the site amplification factor to obtain the peak velocity. Finally, the relation between the peak velocity and instrumental seismic intensity is used to evaluate the seismic intensity on the ground surface. Strong motion is evaluated not in terms of response spectra but in terms of the seismic intensity calculated from the peak velocity.

Seismic hazard maps for specified seismic source faults and long-period ground motion hazard maps are created using certain assumed scenarios and detailed strong motion evaluation. These maps are based on precise predictions of strong ground motions, considering characteristics specific to the earthquake of interest and the ground motion characteristics of the bedrock owing to the three-dimensional subsurface structures in the region. The calculated waveforms are obtained over a broadband frequency range for the engineering bedrock. Because this involves the prediction of strong ground motions for a specific earthquake, PSHA is difficult to apply considering multiple earthquakes with different occurrence times.

The provisional PSHA indicates the probability of strong ground motions occurring within the target period, focusing on the earthquake response spectra of the engineering bedrock. Instead of using the GMPE for the peak velocity in the national seismic hazard maps, the GMPE for response spectra is used. Therefore, strong ground motions can be evaluated probabilistically considering various natural periods. That is, the provisional PSHA evaluates the response spectra of the engineering bedrock using a probabilistic approach. The position of the provisional PSHA with respect to the evaluation method and evaluation target for the ground motion are summarized in Table 1.

Table 1 Position of the provisional PSHA with respect to the evaluation method and evaluation target for the ground motion

| Evaluation method for the ground motion | Evaluation target for the ground motion | |
|---|---|---|
| | Seismic intensity on the ground surface | Response spectra on the engineering bedrock |
| Probabilistic approach | Probabilistic seismic hazard maps | Provisional PSHA |
| Deterministic approach | Seismic hazard maps for specified seismic source faults | Long-period ground motion hazard maps |

## 3. SELECTION OF GMPES FOR RESPONSE SPECTRA

The GMPEs for response spectra were organized, and those for the provisional PSHA were selected in three steps. First, nine GMPEs were selected from recent GMPEs for response spectra. Then, two suitable GMPEs for PSHA within the Japanese context were selected out of the nine. Finally, comparing the predicted values and observed records, the GMPE that has a greater potential to more accurately predict seismic hazards was selected.

### 3.1 Recent GMPEs for response spectra

Douglas[12)] presented a list of approximately 310 GMPEs for response spectra.

In considering the PSHA for Japan, using a GMPE based on many highly accurate strong-motion records is desirable owing to the establishment of high-density strong-motion observation networks all over Japan, such as K-NET[13)], in June 1996. Considering that the effects of subduction-zone earthquakes are significant in many areas of the probabilistic seismic hazard maps[2)], using a GMPE based on strong-motion records of the 2003 Tokachi-oki earthquake, which was the first great interplate earthquake that occurred after the installation of K-NET, is ideal. Additionally, the GMPE must be designed for general use in Japan.

The selection criteria were set based on the above considerations, and nine GMPEs were selected[1], as shown in Table 2.

Table 2 Selection of GMPEs in the first step

| Selection criteria | Selected GMPEs*1 |
|---|---|
| ・ Primarily uses observed records in Japan<br>・ Includes strong-motion records of the 2003 Tokachi-oki earthquake<br>・ Consists of at least 0.1 to 1.0 s periods<br>・ Does not target specific earthquakes or sites<br>・ Published as a peer-reviewed paper | ・ Kanno et al.[14)]<br>・ Zhao et al.[15)]<br>・ Uchiyama and Midorikawa[16)]<br>・ Kataoka et al.[17)]<br>・ Satoh[18), 19)]<br>・ Goda and Atkinson[20)]<br>・ Morikawa and Fujiwara[21)]<br>・ Zhao et al.[22)–25)]<br>・ Sasaki and Ito[26)] |

*1 The GMPEs formulated by Satoh[18)] and Satoh[19)] were treated as one GMPE because the author and data processing methods are the same. Similarly, the GMPEs formulated by Zhao et al.[22)–25)] were treated as a single GMPE.

### 3.2 GMPEs suitable for the PSHA within the Japanese context

Considering the PSHA for Japan, using a GMPE based on strong-motion records of M9-class earthquakes is ideal; it must be applicable to M9-class earthquakes, such as large earthquakes along the Nankai Trough and giant earthquakes along the Japan Trench (off the Pacific coast of Tohoku type). The seismic activity models of the national seismic hazard maps of Japan are developed for shallow earthquakes in land and sea areas (crustal earthquakes) and subduction-zone earthquakes (interplate and intraplate earthquakes), and the excitation characteristics of short-period ground motions can differ depending on the earthquake type. The GMPE should account for the differences in earthquake types when the same seismic activity models as those of the national seismic hazard maps are used. In addition, for deep earthquakes, the GMPE must consider the tendency of the attenuation characteristics of the fore-arc and back-arc sides of the volcanic front to differ.

The selection criteria were set based on the above considerations, and two GMPEs were selected, as shown in Table 3. Hereafter, the GMPE formulated by Morikawa and Fujiwara[21)] is referred to as MF13 and that formulated by Zhao et al.[22)–25)] is referred to as ZZ16.

Table 3 Selection of GMPEs in the second step

| Selection criteria | Selected GMPEs |
|---|---|
| ・ Applicable to M9-class earthquakes<br>・ Considers differences in earthquake types<br>・ Considers the tendency of the attenuation characteristics of the fore-arc and back-arc sides of the volcanic front to differ | ・ Morikawa and Fujiwara[21)] (MF13)<br>・ Zhao et al.[22)–25)] (ZZ16) |

Table 4 summarizes the characteristics of MF13 and ZZ16, focusing on ground-motion intensity, source, attenuation, and site effects. The three points for which the two models differ significantly based on their databases are the attenuation characteristics and the site effects of shallow soft soils and deep

[1] In the provisional PSHA, although GMPEs formulated by Zhao et al.[22)] and Zhao et al.[23)–25)] were treated as different GMPEs in the first step, they were treated together in the second step because the contents of Zhao et al.[22)] were encompassed in Zhao et al.[23)–25)]. These GMPEs were treated together from the first step in this paper to achieve uniformity throughout the selection process.

sediments.

Table 4 Characteristics of MF13 and ZZ16

| GMPE | | MF13 | ZZ16 |
|---|---|---|---|
| Ground-motion intensity | | Vector sum of the time response of two horizontal components | Geometric mean of the maximum response of two horizontal components |
| Source effects | Relation between $M_w$ and the ground motion intensity | Quadratic magnitude term (Model 1) and linear magnitude term (Model 2)[*1] | Linear magnitude term (using quadratic magnitude term together for intraplate earthquakes) |
| | Earthquake types | Crustal earthquake ($M_w$ 5.5–7.9)<br>Interplate earthquake ($M_w$ 5.5–9.0)<br>Intraplate earthquake ($M_w$ 5.5–8.3) | Crustal earthquake ($M_w$ 4.9–7.9)<br>Interplate earthquake ($M_w$ 5.0–9.1)<br>Intraplate earthquake ($M_w$ 5.0–8.3) |
| | Correction term for intraplate earthquakes in the Philippine Sea Plate | Correction term proposed by Morikawa and Fujiwara[27)] [*2] | – |
| Attenuation effects | Equation characteristics | Simpler equations with terms or coefficients related to attenuation less than those in ZZ16 | More complicated equations with terms or coefficients related to attenuation more than those in MF13 |
| | Characteristics of the fore-arc and back-arc sides of the volcanic front | Distance from the volcanic front[29)] and focal depth of the earthquake (shallower than 30 km) | Distance through the volcanic zone[*3] |
| Site effects | Shallow soft soils | Average S-wave velocity up to a depth of 30 m (AVS30) | SC I: AVS30 > 600 m/s<br>SC II: AVS30 = 300–600 m/s<br>SC III: AVS30 = 200–300 m/s<br>SC IV: AVS30 < 200 m/s |
| | Nonlinearity of the ground | – | Considering the nonlinearity of shallow soft soils[*4] |
| | Deep sediments | Top depth of the layer with an S-wave velocity of 1400 m/s | – |

*1 Provisional PSHA used Model 1. Morikawa and Fujiwara[21)] mentioned that the standard deviation of Model 1 was slightly smaller than that of Model 2. Correction terms for amplification by fore-arc/back-arc, shallow soft soils, and deep sediments were proposed only when residual data (residuals between predictions and observations) from Model 1 were used.

*2 Morikawa and Fujiwara[27)] proposed an additional correction term for intraplate earthquakes in the Philippine Sea Plate because of the tendency to overestimate, especially for short periods (approximately < 0.5 s). See Appendix for this paper and Fujiwara et al.[28)].

*3 Based on the original study, the lower and upper limits were set at 12 and 80 km, respectively.

*4 This was not considered in the provisional PSHA.

### 3.3 Selection of GMPEs by comparison of predicted and observed response spectra

Using MF13 and ZZ16, the response spectra were calculated for 23 earthquakes ($M_w$ 5.5–7.1) from January 2013 to May 2021 that were not used in the construction of either GMPE; the residuals were compared with observed records[2].

Figure 1 shows the epicenters of the earthquakes used for comparison. The moment tensors[31)] are also shown. Observation records of the ground surface of K-NET and KiK-net[13)] that met the following criteria were used for comparison:

- Records of observation sites for which AVS30 could be calculated using the method of Midorikawa and Nogi[32)] from the results of PS logging.
- Records of observation sites within 200 km of the shortest distance to the fault,
- Records containing S-wave principal motion confirmed from paste-up waveforms.

Figure 2 shows the residual root mean square ($RMS$) obtained using Eq. (1) for 4,488 records satisfying above three criteria for periods from 0.1 to 5.0 s.

$$RMS = \sqrt{\frac{\sum\{\log(Obs/Pre)\}^2}{n}} \tag{1}$$

where $Obs$: observed record, $Pre$: predicted value, and $n$: number of records.

In Fig. 2, negligible differences were evident for periods shorter than approximately 1.0 s. In contrast, the residuals of MF13 tended to be smaller than those of ZZ16 for periods longer than approximately 1.0 s. Because MF13 considers site effects of deep sediments expressed by the top depth of the layer with an S-wave velocity of 1400 m/s, residuals for periods longer than approximately 1.0 s were considered to be small. MF13 exhibits greater potential to predict seismic hazards more accurately for periods longer than 1.0 s in regions having thick sediments. Thus, MF13 was selected for the provisional PSHA.

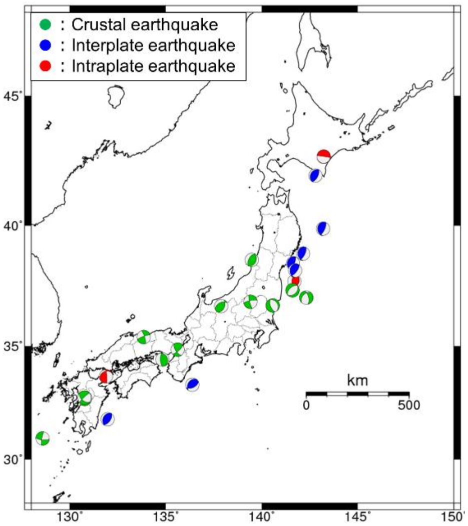


Fig. 1 Epicenters of the earthquakes used for comparison

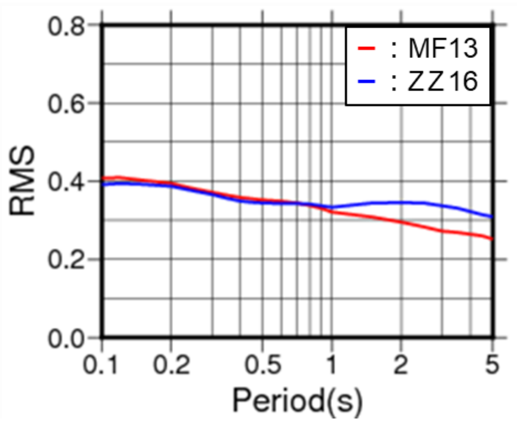


Fig. 2 Root mean square (RMS) of the predicted values and observed records

[2] Comparisons were made for each earthquake type (crustal, interplate, and intraplate earthquakes) considered by MF13 and ZZ16. The 2018 Hokkaido Eastern Iburi Earthquake during the target period covered was not included because different attenuation characters were observed at sites east and west of the epicenter (east side resembles attenuation characters of an interplate earthquake, west side resembles characters of an intraplate earthquake)[30)].

## 4. EVALUATION CONDITIONS FOR THE PSHA OF RESPONSE SPECTRA

### 4.1 GMPE

From MF13, the following equations were used in the provisional PSHA.

$$\log(pre) = a \cdot (M_w{}' - 16.0)^2 + b \cdot X + c - \log\left(X + d \cdot 10^{0.5M_w{}'}\right) + AI + G_d + G_s + PH \quad (2)$$
$$M_w{}' = \min[M_w, 8.2]$$

where $pre$: predicted 5% damped acceleration spectrum (cm/s$^2$), which is calculated as the vector sum of the time responses of the two horizontal components, $M_w, M_w{}'$: moment magnitude, $X$: shortest distance from the source fault to the observation site (km), $a, b, c,$ and $d$: regression coefficients, in which $b$ and $c$ are estimated for each earthquake type (crustal, interplate, and intraplate earthquakes), $PH$: additional correction term for intraplate earthquakes shallower than 80 km in the Philippine Sea Plate[27], $AI$: correction term for anomalous seismic intensity distribution, $G_d$: correction term for the amplification by deep sediments, and $G_s$: correction term for the amplification of shallow soft soils. $AI, G_d,$ and $G_s$ are expressed as follows:

$$AI = \gamma \cdot X_{vf} \cdot (\max[H, 30] - 30) \quad (3)$$
$$G_d = p_d \cdot \log\left(\max\left[D_{l_{min}}, D_{1400}\right]/300\right) \quad (4)$$
$$G_s = p_s \cdot \log\left(\min\left[V_{S_{max}}, AVS30\right]/350\right) \quad (5)$$

In Eq. (3), $X_{vf}$: distance from the volcanic front to the observation site (km), $H$: focal depth of the earthquake (km), and $\gamma$: regression coefficient. In Eq. (4), $D_{1400}$: top depth of the layer with an S-wave velocity of 1400 m/s and $p_d$ $and$ $D_{l_{min}}$: regression coefficients. In Eq. (5), $AVS30$: average S-wave velocity up to a depth of 30 m (m/s) and $p_s$ and $V_{S_{max}}$: regression coefficients. $p_d, D_{l_{min}}, p_s,$ and $V_{S_{max}}$ were used with improved coefficients[28] obtained from Morikawa and Fujiwara[21].

### 4.2 Variance in GMPE

Recent studies have attempted to separate the variance (standard deviation) of ground motions, including the response spectra, into interevent and intraevent variabilities using observed records[33)–37]. However, because research on the variance of ground motions remains insufficient and are still being conducted, the provisional PSHA uses the variance in the National Seismic Hazard Maps for Japan (2020)[2] regardless of the period. Specifically, a variance that depends on the fault distance was adopted for shallow earthquakes in land and sea areas (Eq. (6), Fig. 3 (a)). The amplitude-dependent variance was used for subduction-zone earthquakes (Eq. (7), Fig. 3 (b)).

$$\sigma = \begin{cases} 0.23 & X \le 20 \\ 0.23 - 0.03\dfrac{\log(X/20)}{\log(30/20)} & 20 < X \le 30 \\ 0.20 & X > 30 \end{cases} \quad (6)$$

$$\sigma = \begin{cases} 0.20 & PGV_{b600} \le 25 \\ 0.20 - 0.05\dfrac{PGV_{b600} - 25}{25} & 25 < PGV_{b600} \le 50 \\ 0.15 & PGV_{b600} > 50 \end{cases} \quad (7)$$

where $\sigma$: variance (common logarithmic standard deviation), $X$: shortest distance from the source fault to the observation site (km), and $PGV_{b600}$: peak ground velocity on a stiff ground ($Vs$ = 600 m/s) in Si and Midorikawa[38].

To prevent the ground-motion intensity from becoming unbounded, the skirt of the distribution beyond three times the logarithmic standard deviation (± 3σ) was truncated, as well as the National Seismic Hazard Maps for Japan (2020)[2]. Morikawa et al.[33] estimated the common logarithmic standard deviation from 0.15 to 0.20 when the source area and observation site were fixed. Therefore, the period dependence of the variance was not considered significant.

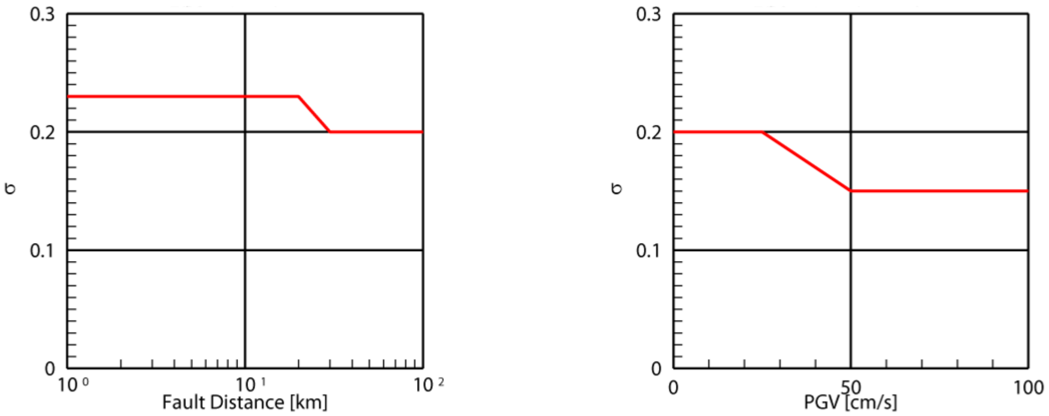


(a) Shallow earthquakes in land and sea areas (Distance-dependent)

(b) Subduction-zone earthquakes (Amplitude-dependent)

Fig. 3 Variance applied in the provisional PSHA (σ: common logarithmic standard deviation)

### 4.3 Evaluation conditions for the provisional PSHA

Focusing on the acceleration spectra, the PSHA was conducted under the following conditions:

- Identical seismic activity models such as those for the National Seismic Hazard Maps for Japan (2020)[2] were used. The probability of an earthquake occurring was set as January 1, 2020.
- Sites of the Tokyo Metropolitan Government Office, Nagoya City Office, and Osaka City Office, which differ in terms of earthquake categories and have high contributions to seismic hazards, were selected. The contribution of subduction-zone earthquakes (especially earthquakes without specified source faults) is significant at the Tokyo Metropolitan Government Office, subduction-zone earthquakes (especially the Nankai Trough earthquake) at the Nagoya City Office, and shallow earthquakes in land and sea areas at the Osaka City Office (detailed in Section 5).
- For relatively shallow intraplate earthquakes without specified source faults in the Philippine Sea Plate, an additional correction term from Morikawa and Fujiwara[27] was applied.
- To promote the utilization of the PSHA of response spectra, the hazard curves, UHS, and contribution factors of the earthquake categories were computed.
- The hazard curves and UHS were computed for the engineered bedrock (AVS30 = 400 m/s).
- Hazard curves were computed for the PE50 for periods of 0.1, 0.5, 1.0, and 5.0 s.
- UHS was computed for eight periods of 0.1, 0.2, 0.3, 0.5, 1.0, 2.0, 3.0, and 5.0 s, corresponding to 39%, 10%, 5%, and 2% PE50 (return periods are approximately 100, 500, 1,000, and 2,500 y, respectively).
- Based on seismic hazard deaggregation, contribution factors were computed for two earthquake categories (shallow earthquakes in land and sea areas and subduction-zone earthquakes). In addition, the contribution factors of detailed earthquake categories (19 categories shown in Table 5) were computed, and the top three categories at any of the eight periods are shown individually, while the other categories are represented as others.

The earthquake categories and correction terms for MF13 are summarized in Table 5.

Table 5 Earthquake categories and correction terms for MF13

| Earthquake categories | Correction terms for MF13 | | |
|---|---|---|---|
| | Earthquake type | Fore-arc /back-arc region | Variance |
| ・ Shallow earthquakes in land and sea areas | Crustal earthquake | — | Distance-dependent |
| ・ Giant earthquakes along the Kuril Trench (17th century type)<br>・ Great interplate earthquakes in Tokachi-Oki<br>・ Great interplate earthquakes in Nemuro-Oki<br>・ Interplate earthquakes close to the offshore trench in the Tokachi-Oki to Etorofuto-Oki regions (tsunami earthquakes, etc.)<br>・ Giant earthquakes along the Japan Trench (off the Pacific coast of Tohoku type)<br>・ Great interplate earthquakes in Aomori-ken-toho-Oki and Northern Iwate-ken-Oki<br>・ Great interplate earthquakes in Miyagi-ken-Oki<br>・ Interplate earthquakes close to the offshore trench in the Aomori-ken-toho-Oki to Boso-Oki regions (tsunami earthquakes, etc.)<br>・ Interplate earthquakes without specified source faults in the Pacific Plate | Interplate earthquake | Northeast Japan | Amplitude-dependent |
| ・ Earthquakes on the seaward side of the Japan Trench axis (outer-rise earthquakes)<br>・ Intraplate earthquakes without specified source faults in the Pacific Plate | Intraplate earthquake | Northeast Japan | Amplitude-dependent |
| ・ Large earthquakes along the Nankai Trough<br>・ M8-class earthquakes along the Sagami Trough*1<br>・ Interplate earthquakes in Hyuganada<br>・ Relatively small interplate earthquakes in Hyuganada<br>・ Earthquakes in the vicinity of Yonaguni-jima<br>・ Interplate earthquakes without specified source faults in the Philippine Sea Plate | Interplate earthquake | Southwest Japan | Amplitude-dependent |
| ・ Intraplate earthquakes without specified source faults in the Philippine Sea Plate*2 | Intraplate earthquake | Southwest Japan | Amplitude-dependent |

*1 Hereafter, this category is referred to as the Sagami Trough Earthquake.
*2 Regarding this category, an additional correction term proposed by Morikawa and Fujiwara[27)] was applied.

## 5. RESULTS OF THE PSHA OF RESPONSE SPECTRA

### 5.1 Tokyo Metropolitan Government Office

Figure 4 shows the hazard curves of the acceleration response spectra for periods of 0.1, 0.5, 1.0, and 5.0 s at the Tokyo Metropolitan Government Office. The vertical axis represents PE50. The hazard curves for all earthquakes (red solid lines) closely overlapped with those of the subduction-zone earthquakes (red dashed lines) at periods of 0.1, 0.5, 1.0, and 5.0 s, indicating that subduction-zone earthquakes made the dominant contribution during the four periods.

Figure 5 shows the UHS of the acceleration response spectra for all earthquakes, shallow earthquakes in land and sea areas, and subduction-zone earthquakes. Curves for 39%, 10%, 5%, and 2% PE50 are shown. The spectral shapes and amplitudes of all earthquakes resemble those of subduction-zone earthquakes, indicating that the dominance of subduction-zone earthquakes extends beyond the specific period points indicated in the hazard curves, encompassing periods of 0.2, 0.3, 2.0, and 3.0 s.

Figure 6 shows the contribution factors of the two earthquake categories. This confirms the dominant contribution of subduction-zone earthquakes.

Figure 7 shows the contribution factors of the detailed earthquake categories. For periods shorter than 0.5 s, the contributions of interplate and intraplate earthquakes without specified source faults in the Philippine Sea Plate tended to be significant. However, for periods longer than 1.0 s, large-magnitude earthquakes at substantial distances from the observation site, such as interplate and intraplate earthquakes without specified source faults in the Pacific Plate, Sagami Trough, and Nankai Trough earthquakes, made significant contributions. This suggests that long-period seismic waves propagate over large distances. In addition, the contribution of Sagami Trough earthquakes was larger for periods of 1.0, 2.0, and 3.0 s at the 2% PE50 (Fig. 7(d)). MF13 tended to have large acceleration response for periods of 1.0 to 3.0 s in the vicinity of source faults (e.g., within approximately 30 km for M8-class earthquakes). The shortest distance from the source faults of the M8-class Sagami Trough earthquakes to the Tokyo Metropolitan Government Office site was approximately 25 km, except for some earthquakes whose source faults were located only off the Boso Peninsula. Therefore, the contribution of the Sagami Trough earthquakes was considered to be larger for periods of 1.0, 2.0, and 3.0 s.

### 5.2 Nagoya City Office

Figure 8 shows the hazard curves of the acceleration response spectra for periods of 0.1, 0.5, 1.0, and 5.0 s at the Nagoya City Office. In addition to the Tokyo Metropolitan Government Office site, the hazard curves for all earthquakes (red solid lines) closely overlapped with those of subduction-zone earthquakes (red dashed lines), indicating that subduction-zone earthquakes made the dominant contribution at periods of 0.1, 0.5, 1.0, and 5.0 s.

Figure 9 shows the UHS of the acceleration response spectra for all earthquakes, shallow earthquakes in land and sea areas, and subduction-zone earthquakes. This indicates that the dominance of subduction-zone earthquakes extends beyond the specific period points indicated in the hazard curves, encompassing periods of 0.2, 0.3, 2.0, and 3.0 s.

Figure 10 shows the contribution factors of the two earthquake categories. This confirms the dominant contribution of subduction-zone earthquakes.

Figure 11 shows the contribution factors of the detailed earthquake categories. The contribution of the Nankai Trough earthquakes was dominant regardless of the PE50 and period. This trend differed from that of the Tokyo Metropolitan Government Office site.

### 5.3 Osaka City Office

Figure 12 shows the hazard curves of the acceleration response spectra for periods of 0.1, 0.5, 1.0, and 5.0 s at the Osaka City Office. In regions with high PE50, the contribution of subduction-zone earthquakes was significant. Conversely, the contribution of shallow earthquakes in land and sea areas tended to be dominant in low-probability regions.

Figure 13 shows the UHS of the acceleration response spectra for all earthquakes, shallow earthquakes in land and sea areas, and subduction-zone earthquakes. For a relatively low PE50, the spectral shapes and amplitudes of all earthquakes resembled those of shallow earthquakes in land and sea areas. Conversely, for a relatively high PE50, particularly for relatively long periods, the spectral shapes and amplitudes of all earthquakes were similar to those of subduction-zone earthquakes.

Figure 14 shows the contribution factors of the two earthquake categories. The contribution of subduction-zone earthquakes increased over longer periods at 39% PE50 (Fig. 14(a)). However, as PE50 decreased, the contribution of shallow earthquakes in land and sea areas tended to be dominant.

Figure 15 shows the contribution factors of the detailed earthquake categories. The contribution of the Nankai Trough earthquakes tended to be significant, particularly for longer periods at 39% PE50 (Fig. 15(a)). However, as PE50 decreases, the contribution of earthquakes occurring in major active fault zones tended to increase, and is especially dominant at 2% PE50. The Uemachi fault zone, a major active fault zone, is located near the Osaka City Office, and the influence of this fault zone is considered significant.

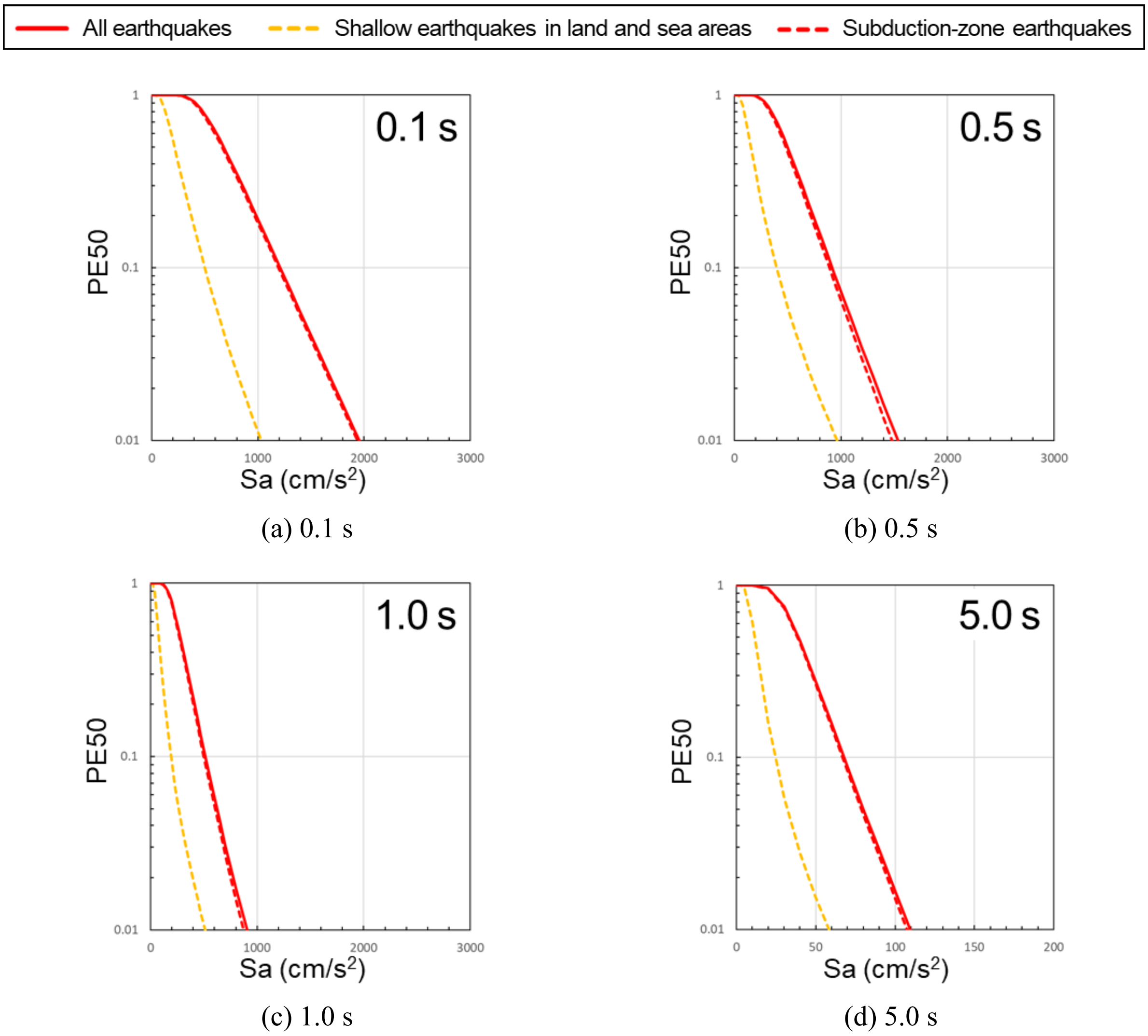


Fig. 4 Hazard curves at the Tokyo Metropolitan Government Office

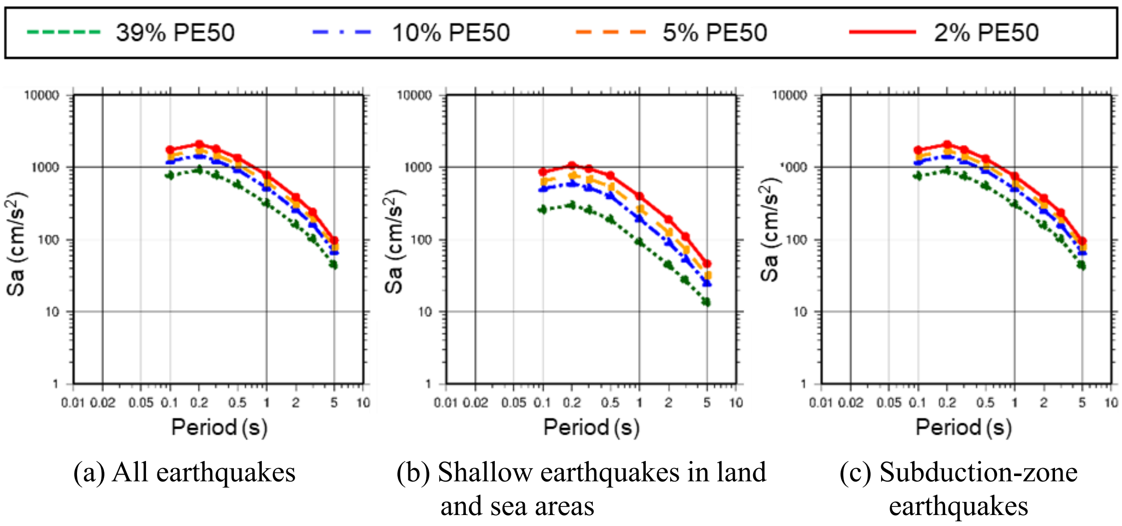


Fig. 5 UHS at the Tokyo Metropolitan Government Office

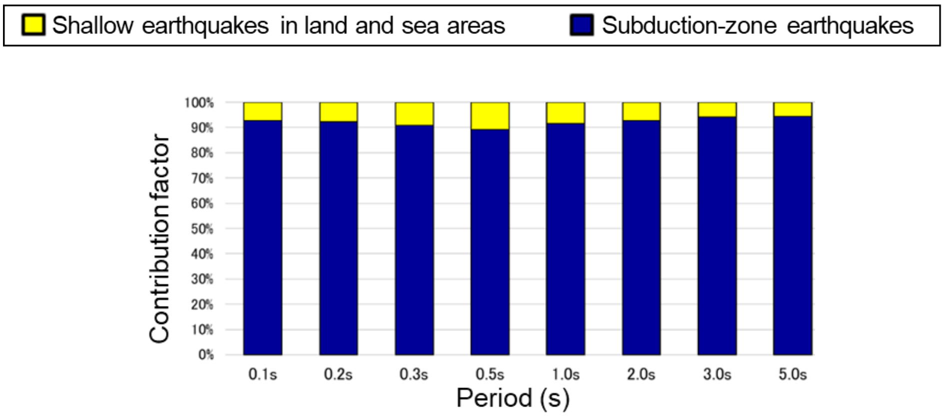


(a) 39% PE50

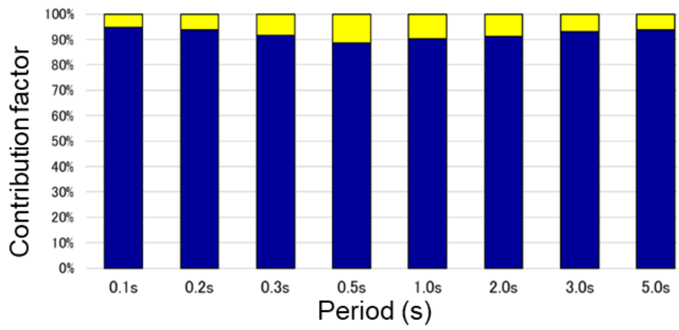


(b) 10% PE50

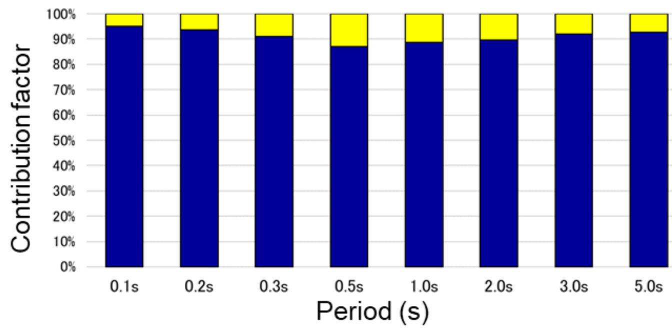


(c) 5% PE50

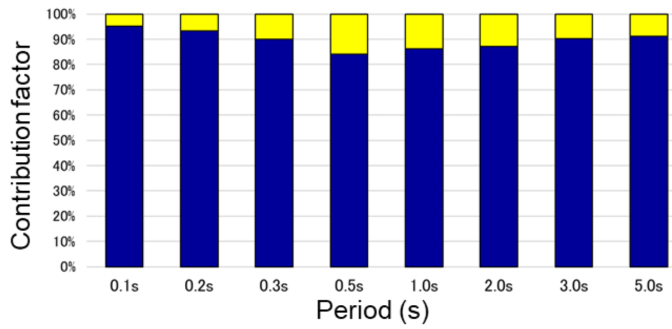


(d) 2% PE50

Fig. 6 Contribution factors of the two earthquake categories at the Tokyo Metropolitan Government Office

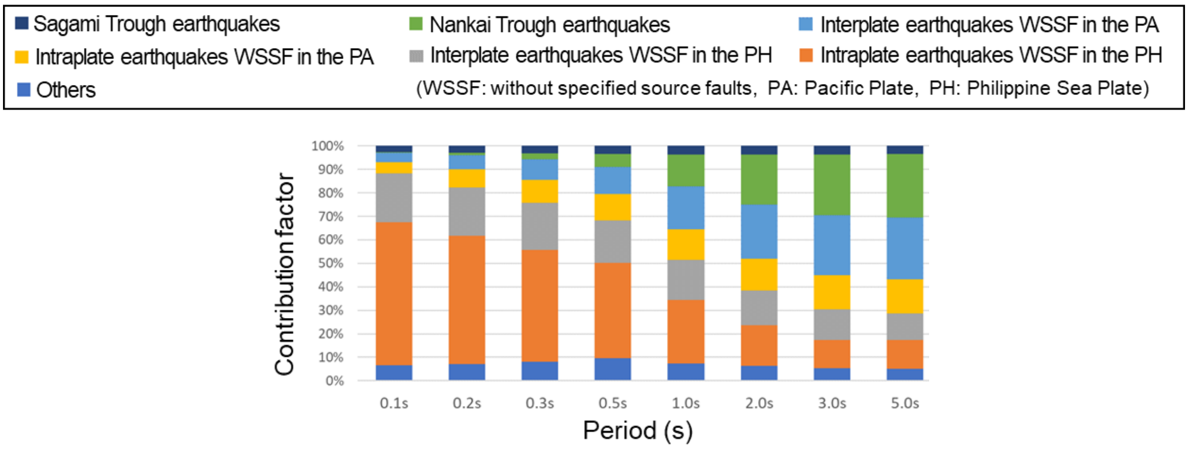


(a) 39% PE50

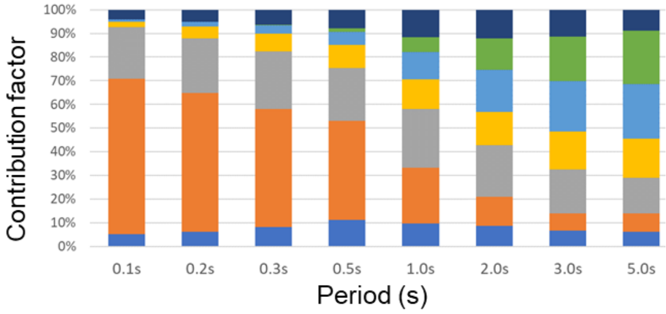


(b) 10% PE50

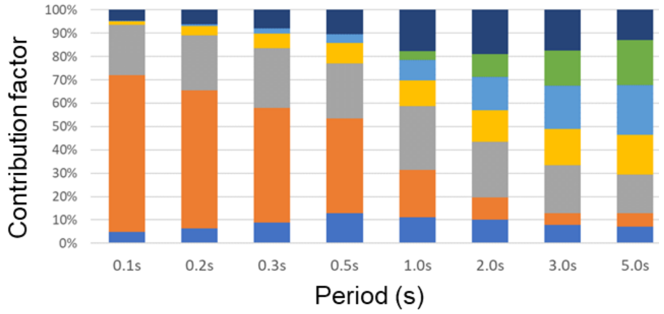


(c) 5% PE50

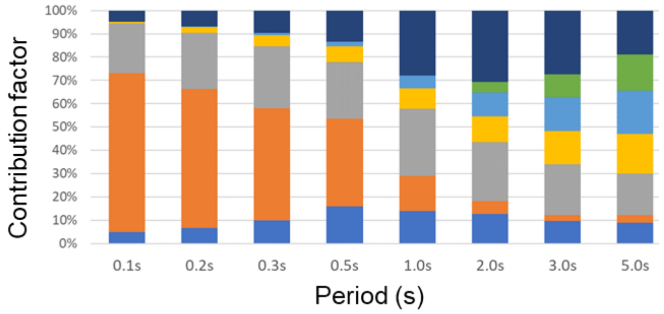


(d) 2% PE50

Fig. 7 Contribution factors of the detailed earthquake categories at the Tokyo Metropolitan Government Office

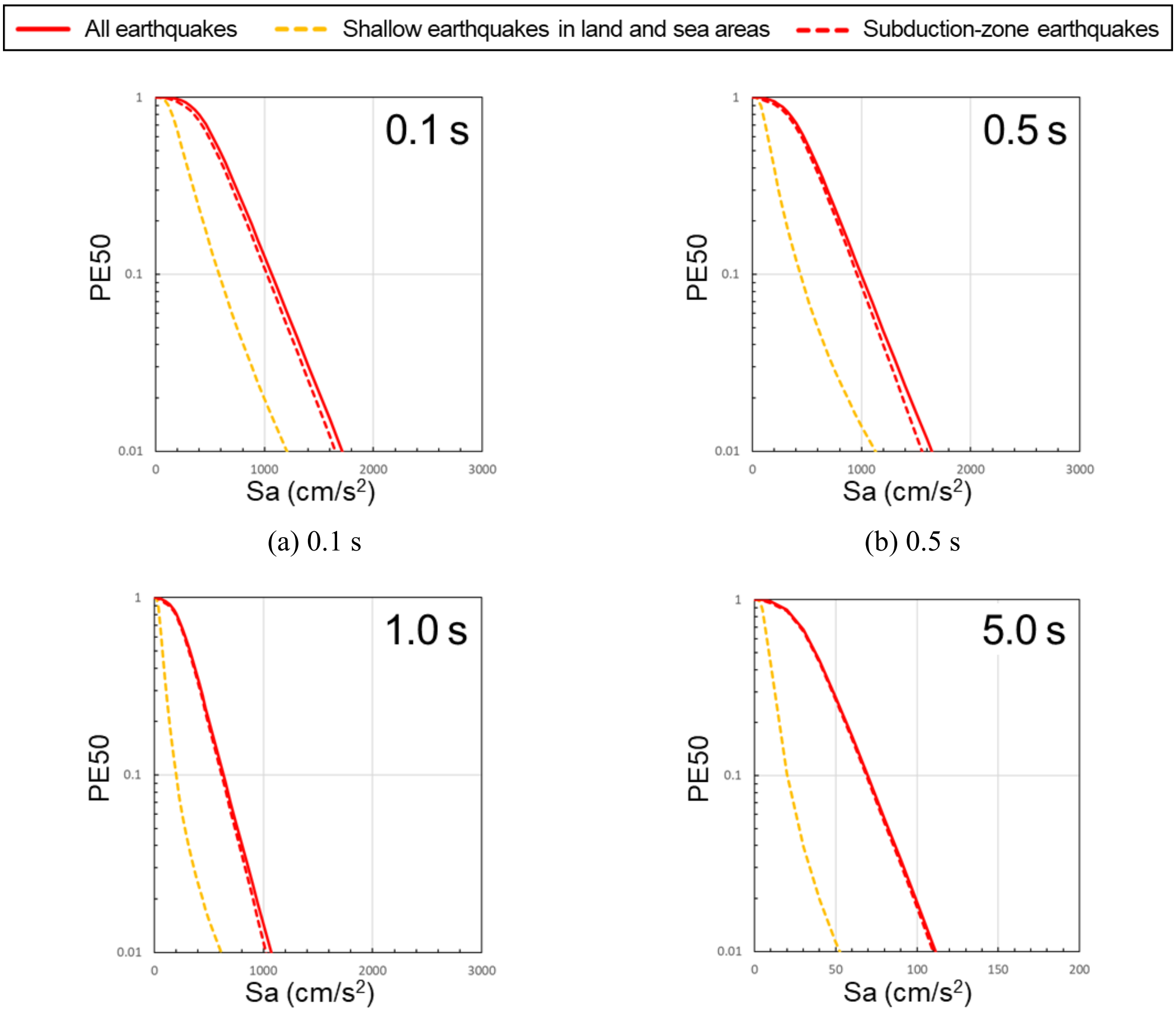


(a) 0.1 s
(b) 0.5 s
(c) 1.0 s
(d) 5.0 s

Fig. 8 Hazard curves at the Nagoya City Office

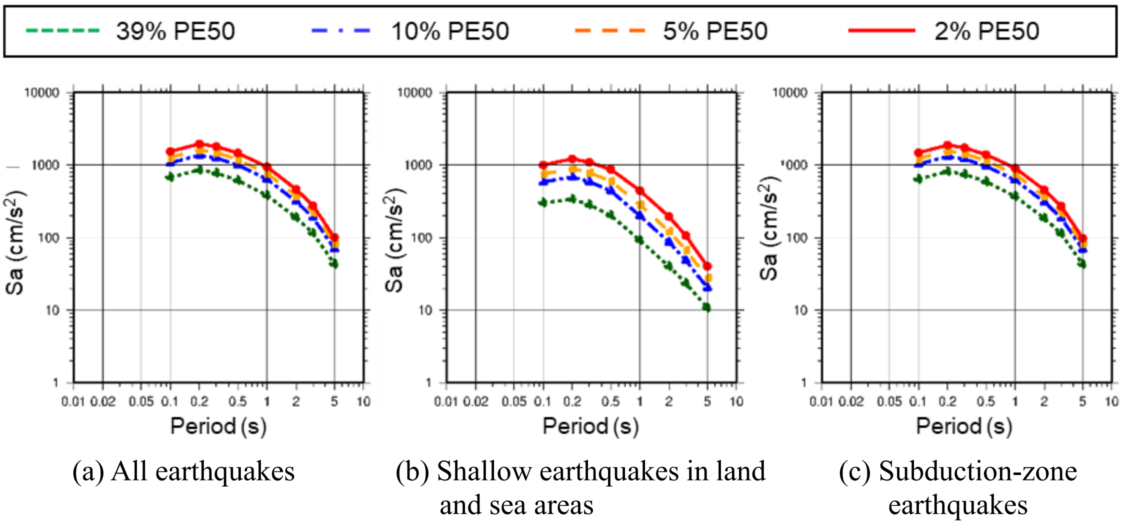


(a) All earthquakes
(b) Shallow earthquakes in land and sea areas
(c) Subduction-zone earthquakes

Fig. 9 UHS at the Nagoya City Office

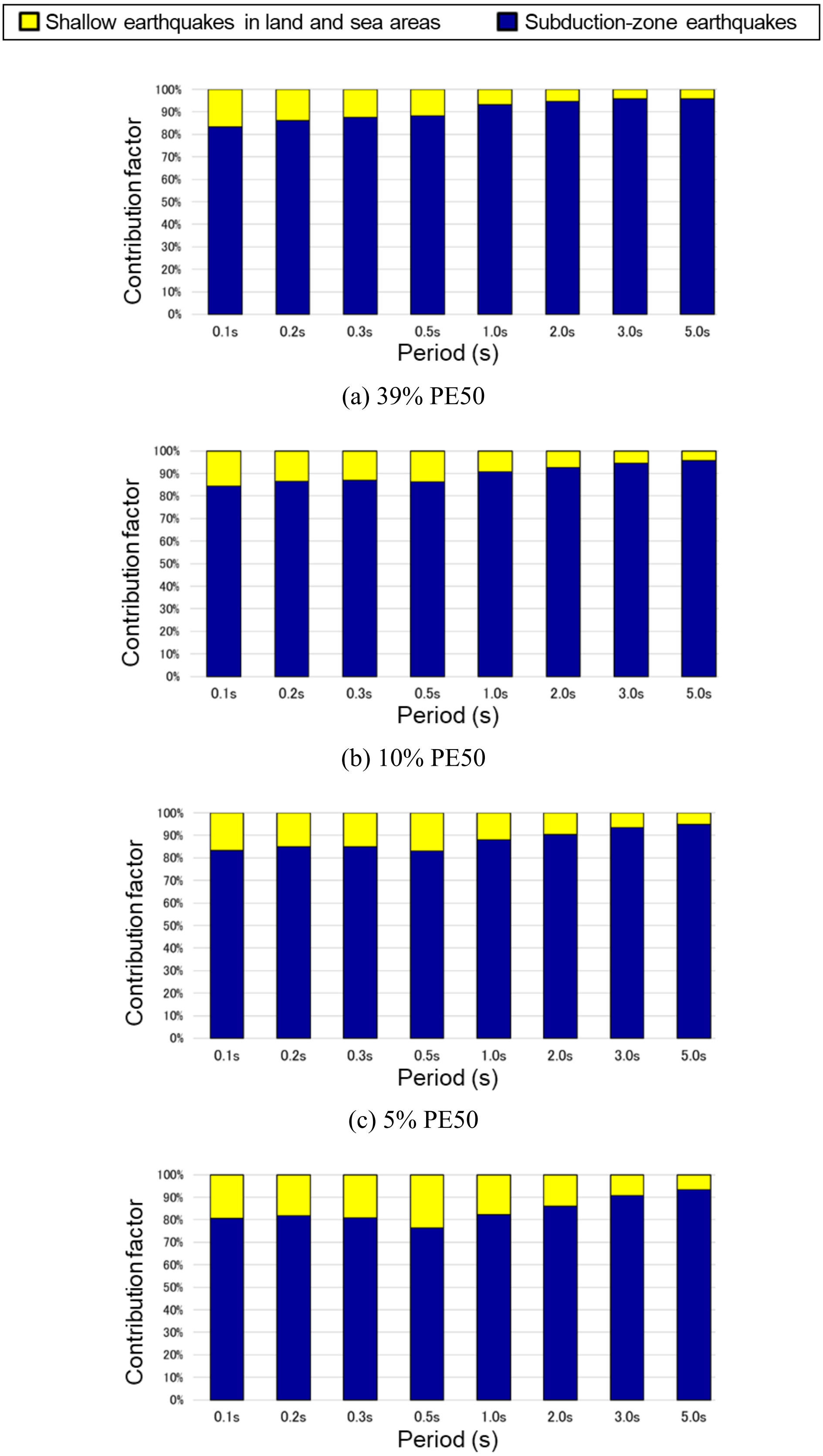


(a) 39% PE50

(b) 10% PE50

(c) 5% PE50

(d) 2% PE50

Fig. 10 Contribution factors of the two earthquake categories at the Nagoya City Office

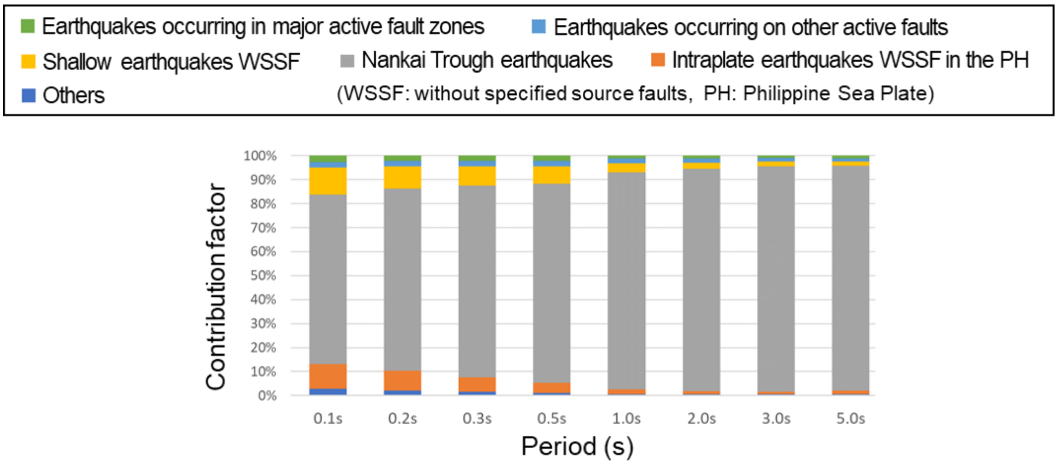


(a) 39% PE50

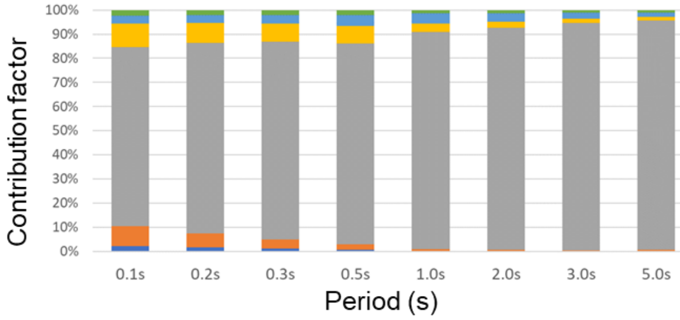


(b) 10% PE50

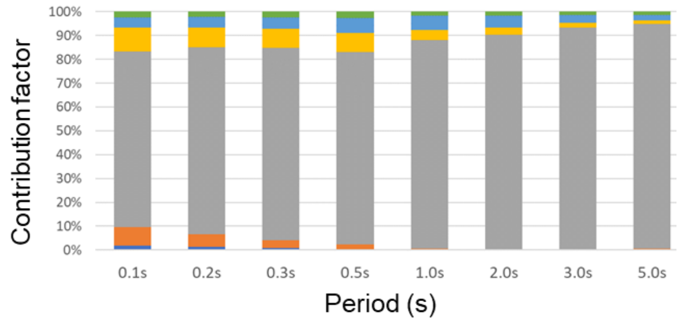


(c) 5% PE50

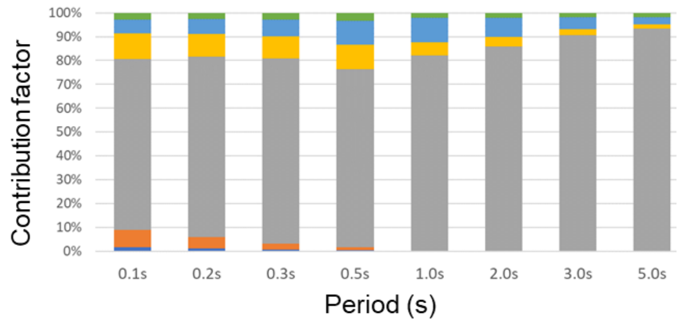


(d) 2% PE50

Fig. 11 Contribution factors of the detailed earthquake categories at the Nagoya City Office

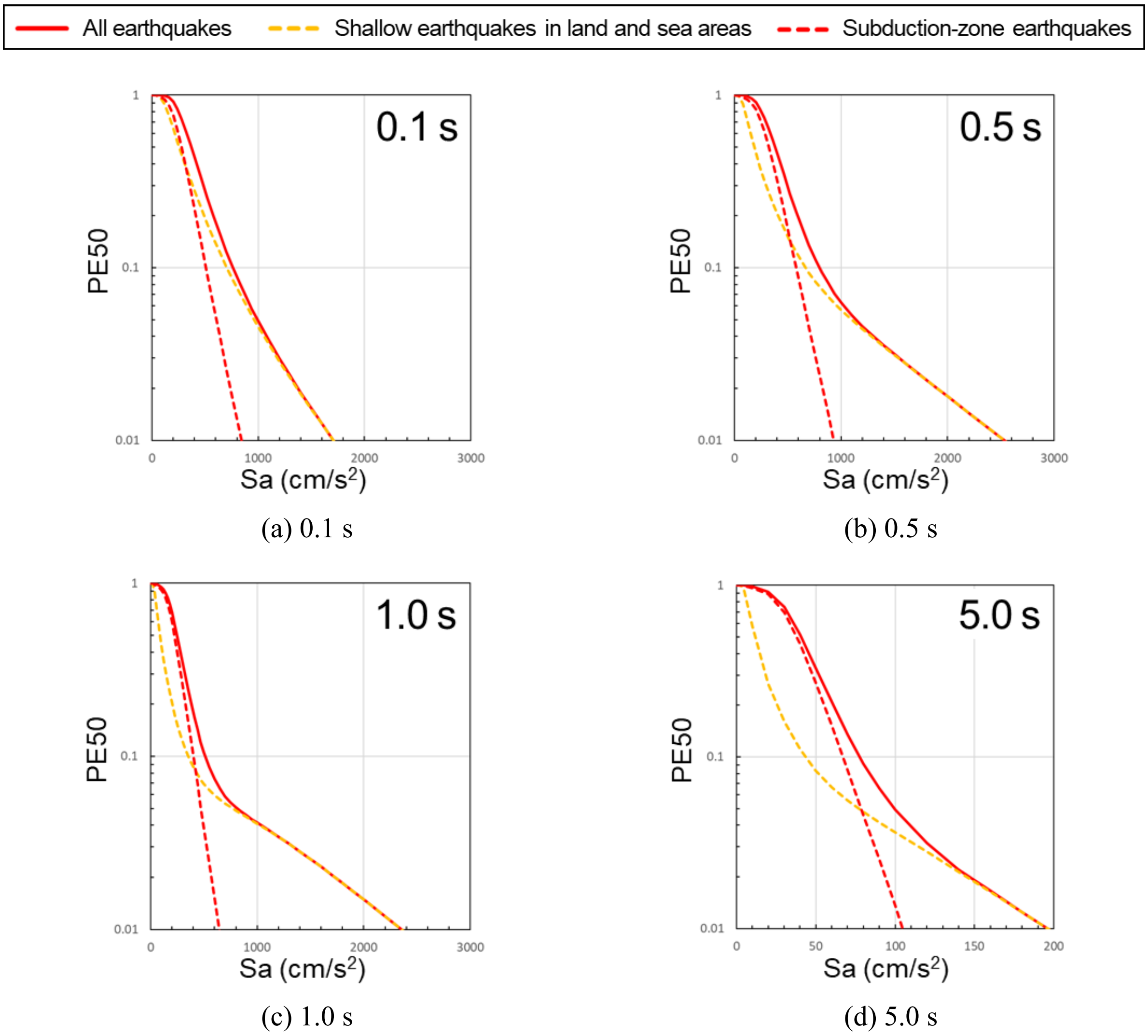


(a) 0.1 s

(b) 0.5 s

(c) 1.0 s

(d) 5.0 s

Fig. 12 Hazard curves at the Osaka City Office

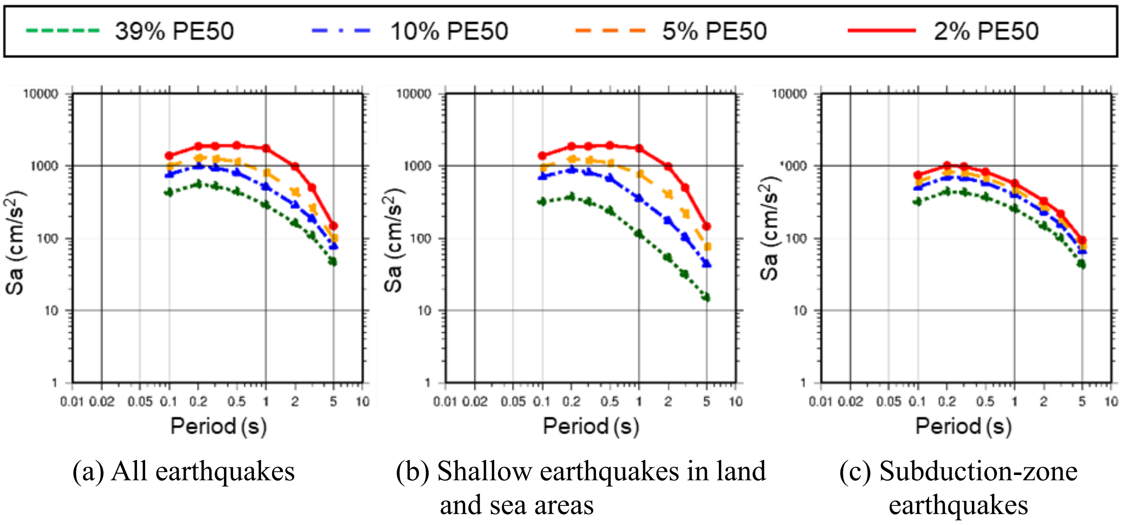


(a) All earthquakes

(b) Shallow earthquakes in land and sea areas

(c) Subduction-zone earthquakes

Fig. 13 UHS at the Osaka City Office

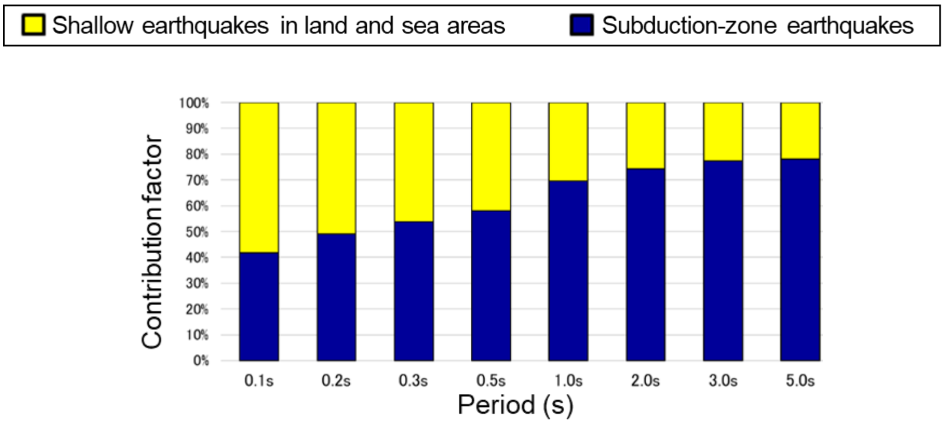


(a) 39% PE50

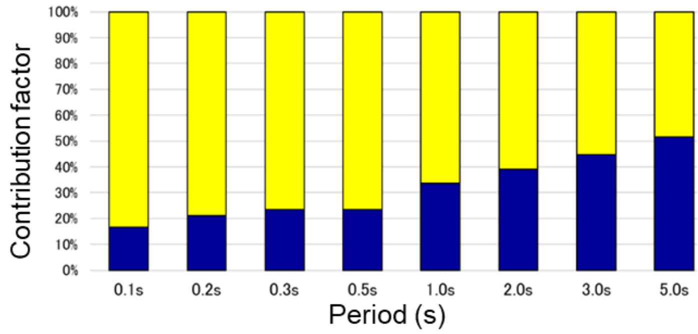


(b) 10% PE50

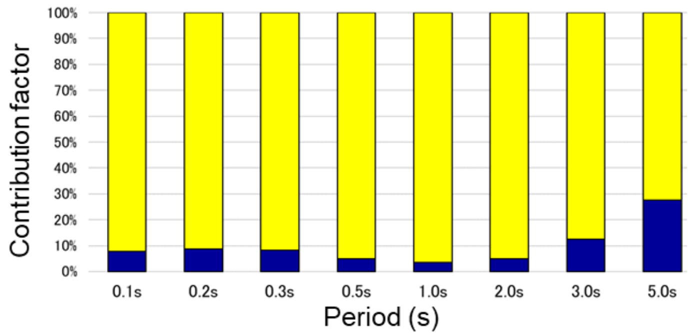


(c) 5% PE50

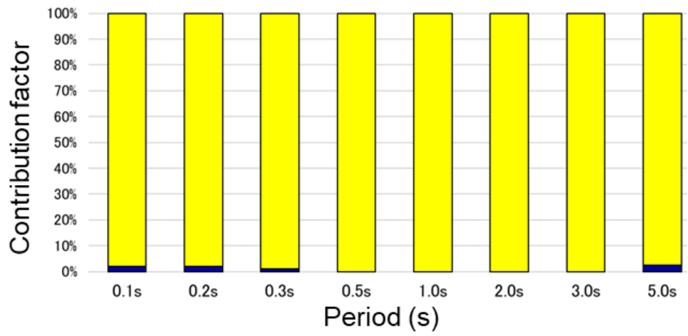


(d) 2% PE50

Fig. 14 Contribution factors of the two earthquake categories at the Osaka City Office

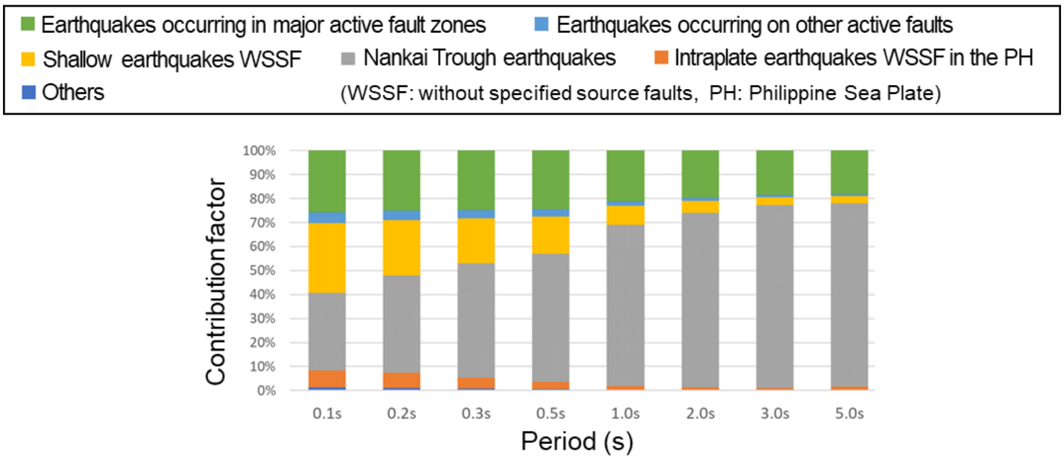


(a) 39% PE50

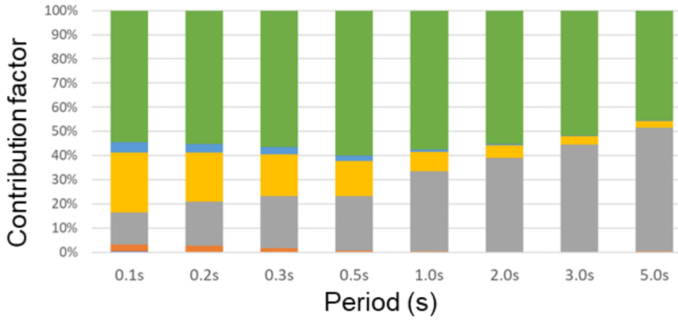


(b) 10% PE50

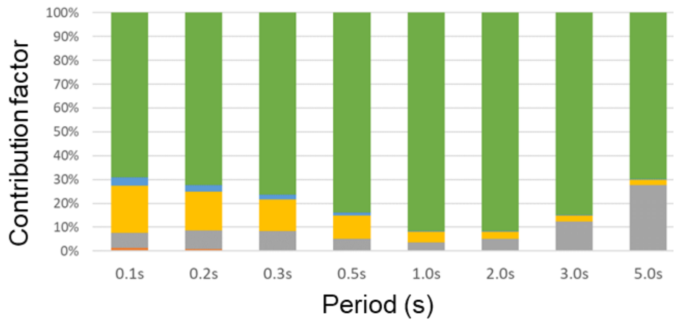


(c) 5% PE50

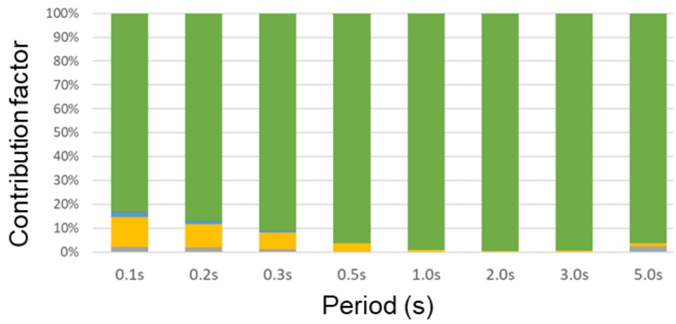


(d) 2% PE50

Fig. 15 Contribution factors of the detailed earthquake categories at the Osaka City Office

## 6. DISCUSSIONS

The provisional PSHA mainly focused on the evaluation conditions and results to contribute to the discussions on the utilization of the PSHA for various needs and improvement of the accuracy of the GMPEs and PSHA. We discuss the utilization of the PSHA of response spectra and the future prospects.

### 6.1 Toward utilization

We anticipate that the continued development of the PSHA of response spectra will contribute to the evaluation of structural seismic responses and the implementation of seismic design according to probability levels, as well as provide useful information for effective countermeasures against earthquake hazards. For example, the following are mentioned in the field of architectural design:

- Selection of construction sites and design policies considering building characteristics and local seismic hazards,
- Selection of earthquake scenarios and comparison of seismic loads for the seismic design of high-rise buildings,
- Consideration of seismic loads in comparison with the design story shear force for medium-low-rise buildings,
- Assessment of business continuity and damage to buildings (economic loss and duration of functional interruption), including nonstructural components and equipment, in addition to structural safety.

In seismic design, including the assessment of nonstructural components and continuous use of buildings, and seismic risk assessment for the business continuity plan (BCP), not only must the low probability be assessed but also the high probability of a seismic hazard. In recent years, digital transformation (DX), which involves the use of various data linked to map information, has become widespread in architectural design, and digital data linked to maps is expected to contribute to its development.

### 6.2 Future prospects

We discuss three aspects for future research: GMPE and PSHA accuracy improvements and utilization.

#### *6.2.1 Concerns in GMPE accuracy improvement*

To improve GMPE accuracy, the datasets on which a GMPE is based must be enriched. This requires the use of data not only from K-NET and KiK-net[13)] but also from the Japan Meteorological Agency, universities, and local public authorities. It also requires continuous maintenance and improvement of strong-motion seismograph networks. Additionally, GMPEs must be constructed based on unified strong-motion databases. In Japan, each researcher constructs GMPEs based on a different database and data-selection criteria; however, GMPEs in other countries, such as the NGA-West2 project in the U.S., are based on a unified database, and the data is selected using the same criteria. Fujiwara et al.[39)] compared the predictions of several GMPEs for Japan and NGA-West2 and showed that the variance of NGA-West2 predictions was smaller. Therefore, a strong-motion database with uniform and comprehensive data must be established in Japan.

#### *6.2.2 Concerns in PSHA accuracy improvement*

To improve PSHA accuracy, the variance of ground motion must be set appropriately. In recent years, with the accumulation of ground motion data, research has been conducted both nationally and internationally regarding the appropriate variance in the PSHA. The magnitude, distance, and period dependence of the variation in the response spectra must be investigated. In addition, because of the limited observational records of giant earthquakes and those in the vicinity of their source fault, a framework for PSHA that allows multiple GMPEs to be considered is necessary to account for epistemic uncertainties.

#### *6.2.3 Concerns in utilization*

The utilization of the PSHA of response spectra requires a discussion with various stakeholders, including those involved in disaster prevention, research, and the construction industry, on how to express and provide evaluation results. For example, for seismic hazard maps based on response spectra, including accessible digital data linked to maps can promote their utilization. Regarding the assessment period, the provisional PSHA showed a exceedance probability of 50 years; however, social requirements may be necessary for the service period of buildings and civil engineering structures may be subject to even longer assessment periods. In terms of period points, more period points may be required for the UHS to be applied to seismic design, ranging from a short period for wooden and medium-low-rise buildings to a long period for high-rise and seismically isolated buildings. For the period band, when the time-history waveform of the ground motion is generated from the UHS, amplitudes of response spectra for periods shorter than 0.1 s and longer than 5.0 s are considered necessary. However, in the long-period band, the influence of the three-dimensional subsurface model is significant, and the accuracy of the current GMPEs may not be sufficient. In addition, seismic hazard information for vertical motion may be useful for the three-dimensional seismic response of buildings, and site amplification factors by period from the engineering bedrock to the ground surface are considered necessary for the PSHA at the ground surface.

## 7. CONCLUSIONS

The Subcommittee for Evaluation of Strong Ground Motion of the ERC published the provisional PSHA for the future utilization of the PSHA in engineering application[8]. This paper reported the position of the provisional PSHA, selection of GMPEs, evaluation conditions, and results for Tokyo, Nagoya, and Osaka. It also discussed how the PSHA can be utilized and its aspects for improvement in the future.

The continued development of the PSHA of response spectra is expected to contribute to structural seismic response evaluation and seismic design implementation according to probability levels, as well as provide useful information for effective countermeasures against earthquake hazards. In addition, discussions with various stakeholders, including those involved in disaster prevention, research, and the construction industry, on the utilization of the PSHA of response spectra are anticipated. In the future, seismic hazard maps of Japan based on response spectra and methods to express and evaluate the PSHA will be discussed.

## ACKNOWLEDGMENT

We thank Dr. Kenichi Kato and Dr. Mitsuko Furumura for their efforts in writing the provisional PSHA and the members of the Subcommittee for Evaluation of Strong Ground Motion and Working Group on Advanced Seismic Hazard Maps for their long-standing discussions on the PSHA of response spectra. We would also like to thank Tatsuya Itoi and other members of the Subcommittee for Seismic Loads on Buildings, Steering Committee for Loads on Buildings, Research Committee on Structures, Architectural Institute of Japan for exchanging opinions on evaluation conditions, expressing evaluation results, and utilizing the PSHA of response spectra. We thank the three anonymous reviewers for their valuable comments. Figure 1 was produced using Generic Mapping Tools (GMT)[40].

## APPENDIX: REGRESSION COEFFICIENTS IN MF13

Table A1 lists the regression coefficients in Eq. (2), and Table A2 lists those in Eqs. (3)–(5). These values are based on Fujiwara et al.[28]

Table A1 Regression coefficients in Eq. (2)

| Period (s) | a | b1 | b2 | b3 | c1 | c2 | c3 | d | PH |
|---|---|---|---|---|---|---|---|---|---|
| 0.1 | −0.0327 | −0.00612 | −0.00606 | −0.00669 | 7.540 | 7.621 | 8.022 | 0.018438 | −0.2470 |
| 0.2 | −0.0321 | −0.00515 | −0.00503 | −0.00548 | 7.431 | 7.479 | 7.872 | 0.011273 | −0.2528 |
| 0.3 | −0.0321 | −0.00454 | −0.00410 | −0.00462 | 7.292 | 7.280 | 7.666 | 0.007670 | −0.2553 |
| 0.5 | −0.0321 | −0.00377 | −0.00283 | −0.00378 | 7.060 | 6.944 | 7.362 | 0.003986 | −0.2564 |
| 1.0 | −0.0327 | −0.00214 | −0.00132 | −0.00233 | 6.628 | 6.475 | 6.861 | 0.000936 | −0.2527 |
| 2.0 | −0.0359 | −0.00160 | −0.00067 | −0.00158 | 6.498 | 6.262 | 6.609 | 0.000703 | −0.2407 |
| 3.0 | −0.0382 | −0.00135 | −0.00051 | −0.00111 | 6.441 | 6.186 | 6.486 | 0.001202 | −0.2288 |
| 5.0 | −0.0393 | −0.00074 | −0.00056 | −0.00116 | 6.147 | 5.896 | 6.182 | 0.002841 | −0.2077 |

b1, c1: Shallow earthquakes in land and sea areas; b2, c2: Interplate earthquakes; b3, c3: Intraplate earthquakes

Table A2 Regression coefficients in Eqs. (3)–(5)

| Period (s) | pd | Dlmin | ps | Vsmax | γNE | γSW |
|---|---|---|---|---|---|---|
| 0.1 | −0.084855 | 15.0 | −0.284416 | 2000.0 | 0.000083913 | 0.000065915 |
| 0.2 | −0.043392 | 15.0 | −0.633661 | 2000.0 | 0.000080150 | 0.000065410 |
| 0.3 | −0.019984 | 15.0 | −0.793002 | 2000.0 | 0.000077949 | 0.000065114 |
| 0.5 | 0.030246 | 15.0 | −0.891130 | 1900.0 | 0.000070750 | 0.000064742 |
| 1.0 | 0.128832 | 15.0 | −0.778652 | 1482.4 | 0.000053238 | 0.000045076 |
| 2.0 | 0.253945 | 33.7 | −0.543585 | 1156.6 | 0.000035726 | 0.000018572 |
| 3.0 | 0.323118 | 57.8 | −0.413921 | 1000.3 | 0.000025482 | 0.000003068 |
| 5.0 | 0.419676 | 113.8 | −0.294664 | 833.1 | 0.000015238 | −0.000012435 |

γNE: Earthquakes in the Pacific Plate, γSW: Earthquakes in the Philippine Sea Plate

## REFERENCES


1) Earthquake Research Committee, the Headquarters for Earthquake Research Promotion: National Seismic Hazard Maps for Japan (2005), 2005. https://www.jishin.go.jp/main/index-e.html (last accessed on January 31, 2023)
2) Earthquake Research Committee, the Headquarters for Earthquake Research Promotion: National Seismic Hazard Maps for Japan (2020), 2021 (in Japanese). https://www.jishin.go.jp/evaluation/seismic_hazard_map/shm_report/shm_report_2020/ (last accessed on January 31, 2023)
3) Shumway, A. M., Clayton, B. S. and Rukstales, K. S.: Data Release for Additional Period and Site Class Data for the 2018 National Seismic Hazard Model for the Conterminous United States (ver. 1.2, May 2021), *U.S. Geological Survey Data Release*, 2021. https://doi.org/10.5066/P9RQMREV
4) Powers, P. M., Rezaeian, S., Shumway, A. M., Petersen, M. D., Luco, N., Boyd, O. S., Moschetti, M. P., Frankel, A. D. and Thompson, E. M.: The 2018 Update of the US National Seismic Hazard Model: Ground Motion Models in the Western US, *Earthquake Spectra*, Vol. 37, No. 4, pp. 2315–2341, 2021. https://doi.org/10.1177/87552930211011200
5) Danciu, L., Nandan, S., Reyes, C., Basili, R., Weatherill, G., Beauval, C., Rovida, A., Vilanova, S., Sesetyan, K., Bard, P.-Y., Cotton, F., Wiemer, S. and Giardini, D.: The 2020 Update of the European Seismic Hazard Model: Model Overview, *EFEHR Technical Report 001*, v1.0.0, 2021. https://doi.org/10.12686/a15
6) Gerstenberger, M. C., Bora, S., Bradley, B. A., DiCaprio, C., Van Dissen, R. J., Atkinson, G. M.,

Chamberlain, C., Christophersen, A., Clark, K. J., Coffey, G. L., de la Torre, C. A., Ellis, S. M., Fraser, J., Graham, K. and Griffin, J.: New Zealand National Seismic Hazard Model 2022 Revision: Model, Hazard and Process Overview, *GNS Science*, 2022. https://doi.org/10.21420/TB83-7X19
7) Headquarters for Earthquake Research Promotion: The Promotion of Earthquake Research: Basic Comprehensive Policy for the Promotion of Earthquake Observation, Measurement, Surveys and Research (Third Period), 2019 (in Japanese). https://www.jishin.go.jp/main/suihon/honbu19b/suishin190531.pdf (last accessed on January 31, 2023)
8) Subcommittee for Evaluation of Strong Ground Motion, the Earthquake Research Committee, the Headquarters for Earthquake Research Promotion: Probabilistic Seismic Hazard Analysis of Response Spectra (provisional edition), 2022 (in Japanese, title translated by the authors). https://www.jishin.go.jp/evaluation/seismic_hazard_map/sh_response_spectrum/ (last accessed on January 31, 2023)
9) Earthquake Research Committee, the Headquarters for Earthquake Research Promotion: Long-Period Ground Motion Hazard Map (provisional edition 2009), 2009 (in Japanese, title translated by the authors). https://www.jishin.go.jp/evaluation/seismic_hazard_map/lpshm/09_choshuki/ (last accessed on January 31, 2023)
10) Earthquake Research Committee, the Headquarters for Earthquake Research Promotion: Long-Period Ground Motion Hazard Map (provisional edition 2012), 2012 (in Japanese, title translated by the authors). https://www.jishin.go.jp/evaluation/seismic_hazard_map/lpshm/12_choshuki/ (last accessed on January 31, 2023)
11) Earthquake Research Committee, the Headquarters for Earthquake Research Promotion: Long-Period Ground Motion Hazard Map for Great Earthquakes along the Sagami Trough (provisional edition 2016), 2016 (in Japanese, title translated by the authors). https://www.jishin.go.jp/evaluation/seismic_hazard_map/lpshm/16_choshuki/ (last accessed on January 31, 2023)
12) Douglas, J.: Ground Motion Prediction Equations 1964–2021, 2022. http://www.gmpe.org.uk/gmpereport2014.pdf (last accessed on July 1, 2023)
13) National Research Institute for Earth Science and Disaster Resilience: *NIED K-NET*, *KiK-net*, National Research Institute for Earth Science and Disaster Resilience, 2019. https://doi.org/10.17598/NIED.0004
14) Kanno, T., Narita, A., Morikawa, N., Fujiwara, H. and Fukushima, Y.: A New Attenuation Relation for Strong Ground Motion in Japan Based on Recorded Data, *Bulletin of the Seismological Society of America*, Vol. 96, No. 3, pp. 879–897, 2006. https://doi.org/10.1785/0120050138
15) Zhao, J. X., Irikura, K., Zhang, J., Fukushima, Y., Somerville, P. G., Asano, A., Ohno, Y., Oouchi, T., Takahashi, T. and Ogawa, H.: An Empirical Site-Classification Method for Strong-Motion Stations in Japan Using H/V Response Spectral Ratio, *Bulletin of the Seismological Society of America*, Vol. 96, pp. 914–925, 2006. https://doi.org/10.1785/0120050124
16) Uchiyama, Y. and Midorikawa, S.: Attenuation Relationship for Response Spectra on Engineering Bed Rock Considering Effects of Focal Depth, *Journal of Structural and Construction Engineering*, Vol. 71, No. 606, pp. 81–88, 2006 (in Japanese). https://doi.org/10.3130/aijs.71.81_2
17) Kataoka, S., Satoh, T., Matsumoto, S. and Kusakabe, T.: Attenuation Relationships of Ground Motion Intensity Using Short Period Level as a Variable, *Doboku Gakkai Ronbunshuu A*, Vol. 62, No. 4, pp. 740–757, 2006 (in Japanese). https://doi.org/10.2208/jsceja.62.740
18) Satoh, T.: Attenuation Relations of Horizontal and Vertical Ground Motions for P Wave, S Wave, and All Duration of Crustal Earthquakes, *Journal of Structural and Construction Engineering*, Vol. 73, No. 632, pp. 1745–1754, 2008 (in Japanese). https://doi.org/10.3130/aijs.73.1745
19) Satoh, T.: Attenuation Relations of Horizontal and Vertical Ground Motions for Intraslab and Interplate Earthquakes in Japan, *Journal of Structural and Construction Engineering*, Vol. 75, No. 647, pp. 67–76, 2010 (in Japanese). https://doi.org/10.3130/aijs.75.67
20) Goda, K. and Atkinson, G. M.: Probabilistic Characterization of Spatially Correlated Response Spectra for Earthquakes in Japan, *Bulletin of the Seismological Society of America*, Vol. 99, No. 5, pp. 3003–3020, 2009. https://doi.org/10.1785/0120090007

21) Morikawa, N. and Fujiwara, H.: A New Ground Motion Prediction Equation for Japan Applicable up to M9 Mega-Earthquake, *Journal of Disaster Research*, Vol. 8, No. 5, pp. 878–888, 2013. https://doi.org/10.20965/jdr.2013.p0878
22) Zhao, J. X., Zhou, S., Gao, P., Long, T., Zhang, Y., Thio, H. K., Lu, M. and Rhoades, D. A.: An Earthquake Classification Scheme Adapted for Japan Determined by the Goodness of Fit for Ground-Motion Prediction Equations, *Bulletin of the Seismological Society of America*, Vol. 105, No. 5, pp. 2750–2763, 2015. https://doi.org/10.1785/0120150013
23) Zhao, J. X., Liang, X., Jiang, F., Xing, H., Zhu, M., Hou, R., Zhang, Y., Lan, X., Rhoades, D. A., Irikura, K., Fukushima, Y. and Somerville, P. G.: Ground-Motion Prediction Equations for Subduction Interface Earthquakes in Japan Using Site Class and Simple Geometric Attenuation Functions, *Bulletin of the Seismological Society of America*, Vol. 106, No. 4, pp. 1518–1534, 2016. https://doi.org/10.1785/0120150034
24) Zhao, J. X., Jiang, F., Shi, P., Xing, H., Huang, H., Hou, R., Zhang, Y., Yu, P., Lan, X., Rhoades, D. A., Somerville, P. G., Irikura, K. and Fukushima, Y.: Ground-Motion Prediction Equations for Subduction Slab Earthquakes in Japan Using Site Class and Simple Geometric Attenuation Functions, *Bulletin of the Seismological Society of America*, Vol. 106, No. 4, pp. 1535–1551, 2016. https://doi.org/10.1785/0120150056
25) Zhao, J. X., Zhou, S., Zhou, J., Zhao, C., Zhang, H., Zhang, Y., Gao, P., Lan, X., Rhoades, D. A., Fukushima, Y., Somerville, P. G. and Irikura, K.: Ground-Motion Prediction Equations for Shallow Crustal and Upper-Mantle Earthquakes in Japan Using Site Class and Simple Geometric Attenuation Functions, *Bulletin of the Seismological Society of America*, Vol. 106, No. 4, pp. 1552–1569, 2016. https://doi.org/10.1785/0120150063
26) Sasaki, T. and Ito T.: Attenuation Relationship of Earthquake Motion at Dam Foundation in Consideration of Tohoku Earthquake, *Journal of Japan Association for Earthquake Engineering*, Vol. 16, No. 4, pp. 80–92, 2016 (in Japanese). https://doi.org/10.5610/jaee.16.4_80
27) Morikawa, N. and Fujiwara, H.: An Additional Correction Term of Ground-Motion Prediction Equation for Intra-Plate Earthquakes, *Japan Geoscience Union Meeting 2015*, Chiba, Japan, SSS25-14, 2015 (in Japanese).
28) Fujiwara, H., Morikawa, N., Maeda, T., Iwaki, A., Senna, S., Kawai, S., Azuma, H., Hao, K. X., Imoto, M., Wakamatsu, K., Miyakoshi, J., Morii, T., Shimazu, N., Takahashi, M. and Akatsuka, M.: Improved Seismic Hazard Assessment after the 2011 Great East Japan Earthquake (Part 2), *Technical Note of the National Research Institute for Earth Science and Disaster Resilience*, No. 489, 391 pp., 2023 (in Japanese). https://doi.org/10.24732/NIED.00003933
29) Fujiwara, H., Morikawa, N., Kawai, S., Aoi, S., Senna, S., Maeda, T., Azuma, H., Hao, K. X., Iwaki, A., Wakamatsu, K., Imoto, M., Hasegawa, N., Okumura, T., Hayakawa, T. and Takahashi, M.: Improved Seismic Hazard Assessment after the 2011 Great East Japan Earthquake, *Technical Note of the National Research Institute for Earth Science and Disaster Resilience*, No. 399, 253 pp., 2015 (in Japanese). http://doi.org/10.24732/nied.00002013
30) Matsu'ura, R. S., Tanaka, H., Furumura, M. and Takahama, T.: The Unique Characters of Intensity Distribution of the 2018 Sep. 6 Mw6.6 Earthquake of Iburi Region in Hokkaido, Japan, *Japan Geoscience Union Meeting 2019*, Chiba, Japan, SSS10-P17, 2019 (in Japanese).
31) National Research Institute for Earth Science and Disaster Resilience: *NIED F-net*, National Research Institute for Earth Science and Disaster Resilience, 2019. https://doi.org/10.17598/NIED.0005
32) Midorikawa, S. and Nogi, Y.: Estimation of VS30 from Shallow Velocity Profile, *Journal of Japan Association for Earthquake Engineering*, Vol. 5, No. 2, pp. 91–96, 2015 (in Japanese). https://doi.org/10.5610/jaee.15.2_91
33) Morikawa, N., Kanno, T., Narita, A., Fujiwara, H., Okumura, T., Fukushima, Y. and Guerpinar, A.: Strong Motion Uncertainty Determined from Observed Records by Dense Network in Japan, *Journal of Seismology*, Vol. 12, No. 4, pp. 529–546, 2008. https://doi.org/10.1007/s10950-008-9106-2
34) Rodriguez-Mark, A., Montalva, G. A., Cotton, F. and Bonilla, F.: Analysis of Single-Station Standard Deviation Using the KiK-net Data, *Bulletin of Seismological Society of America*, Vol. 101,

No. 3, pp. 1242–1258, 2011. https://doi.org/10.1785/0120100252
35) Lin, P. S., Chiou, B., Abrahamson, N., Walling, M., Lee, C. T. and Cheng, C. T.: Repeatable Source, Site, and Path Effects on the Standard Deviation for Empirical Ground-Motion Prediction Models, *Bulletin of Seismological Society of America*, Vol. 101, No. 5, pp. 2281–2295, 2011. https://doi.org/10.1785/0120090312
36) Hikita, T. and Tomozawa, Y.: Variation of Ground Motion Response Spectra Based on Pair Ground Motion Records Observed at the Same Site from Two Earthquakes with the Same Magnitude and Hypocenter Location, *Journal of Structural and Construction Engineering*, Vol. 78, No. 686, pp. 723–732, 2013 (in Japanese). https://doi.org/10.3130/aijs.78.723
37) Villani, M. and Abrahamson, N. A.: Repeatable Site and Path Effects on the Ground-Motion Sigma Based on Empirical Data from Southern California and Simulated Waveforms from the Cybershake Platform, *Bulletin of Seismological Society of America*, Vol. 105, No. 5, pp. 2681–2695, 2015. https://doi.org/10.1785/0120140359
38) Si, H. and Midorikawa, S: New Attenuation Relationships for Peak Ground Acceleration and Velocity Considering Effects of Fault Type and Site Condition, *Journal of Structural and Construction Engineering*, Vol. 64, No. 523, pp. 63–70, 1999 (in Japanese). https://doi.org/10.3130/aijs.64.63_2
39) Fujiwara, H., Ebisawa, K., Kagawa, T., Si, H., Furumura, T., Miyake, H., Morikawa, N., Shiota, T., Ogawa, H., Matsusaki, S., Miyakoshi, J., Sakai, T. and Kameda, H.: Development of Ground Motion Characterization Model at the Ikata Site Based on Guidelines for SSHAC Level 3, *Journal of Japan Association for Earthquake Engineering*, Vol. 22, No. 2, pp. 61–87, 2022 (in Japanese). https://doi.org/10.5610/jaee.22.2_61
40) Wessel, P. and Smith, W. H. F.: New, Improved Version of Generic Mapping Tools Released, *Eos, Transactions American Geophysical Union*, Vol. 79, No. 47, p. 579, 1998. https://doi.org/10.1029/98EO00426

**(Original Japanese Paper Published: February, 2024)**
**(English Version Submitted: March 28, 2024)**
**(English Version Accepted: June 17, 2024)**